

TECHNICAL REPORT

DIMITRA paediatric skull phantoms: development of age-specific paediatric models for dentomaxillofacial radiology research

^{1,2}Anne Caroline Oenning, ¹Benjamin Salmon, ^{2,3}Karla de Faria Vasconcelos, ³Laura Ferreira Pinheiro Nicolielo, ⁴Ivo Lambrichts, ⁵Gerard Sanderink, ^{3,6}Ruben Pauwels, ⁷DIMITRA Group and ^{3,8}Reinhilde Jacobs

¹Department of Dental Medicine, Orofacial Pathologies Imaging and Biotherapies Lab, Paris Descartes University Sorbonne Paris Cité, Bretonneau Hospital, Paris, France; ²Department of Oral Diagnosis, Division of Oral Radiology, Piracicaba Dental School, University of Campinas, Piracicaba, Sao Paulo, Brazil; ³Department of Imaging and Pathology, OMFS IMPATH research group, Catholic University of Leuven, University Hospitals Leuven, Leuven, Belgium; ⁴Department of Morphology, Biomedical Research Institute, University of Hasselt, Hasselt, Belgium; ⁵Department of Oral Radiology, Academic Center for Dentistry Amsterdam, University of Amsterdam and Vrije Universiteit, Amsterdam, Netherlands; ⁶Department of Radiology, Faculty of Dentistry, Chulalongkorn University, Bangkok, Thailand; ⁷DIMITRA group available at www.dimitra.be, Leuven, Belgium; ⁸Department of Dental Medicine, Karolinska Institutet, Stockholm, Sweden

Objectives: This report aims to describe the development of age-specific phantoms for use in paediatric dentomaxillofacial radiology research. These phantoms are denoted DIMITRA paediatric skull phantoms as these have been primarily developed and validated for the DIMITRA European research project (*Dentomaxillofacial paediatric imaging: an investigation towards low-dose radiation induced risks*).

Methods: To create the DIMITRA paediatric phantoms, six human paediatric skulls with estimated ages ranging between 4 and 10 years-old were selected, protected with non-radiopaque tape and immersed in melted Mix-D soft tissue equivalent material, by means of a careful procedure (layer-by-layer). Mandibles were immersed separately and a Mix-D tongue model was also created. For validation purposes, the resulting paediatric phantoms were scanned using a cone-beam CT unit with different exposure parameter settings.

Results: Preliminary images deriving from all scans were evaluated by two dentomaxillofacial radiologists, to check for air bubbles, artefacts and inhomogeneities of the Mix-D and a potential effect on the visualization of the jaw bone. Only skulls presenting perfect alignment of Mix-D surrounding the bone surfaces with adequate and realistic soft tissue thickness density were accepted.

Conclusions: The DIMITRA anthropomorphic phantoms can yield clinically equivalent images for optimization studies in dentomaxillofacial research. In addition, the layer-by-layer technique proved to be practical and reproducible, as long as recommendations are carefully followed.

Dentomaxillofacial Radiology (2018) 47, 20170285. doi: [10.1259/dmfr.20170285](https://doi.org/10.1259/dmfr.20170285)

Cite this article as: Oenning AC, Salmon B, Vasconcelos KdF, Pinheiro Nicolielo LF, Lambrichts I, Sanderink G, et al. DIMITRA paediatric skull phantoms: development of age-specific paediatric models for dentomaxillofacial radiology research. *Dentomaxillofac Radiol* 2018; 47: 20170285.

Keywords: cone-beam computed tomography; paediatric dentistry; radiation protection; imaging phantoms

Introduction

It is well known that for each specific cone-beam CT (CBCT) scan, the exposure protocol should ideally consider both patient-specific features and indication-oriented requirements in order to obtain dose reduction at a satisfactory image quality level based on ALADA (as low as diagnostically acceptable)¹ and ALADAIP (as low as diagnostically acceptable being indication-oriented and patient-specific).² Considering the large variety of technical parameters available on each CBCT device, suitable protocols should become more specific and controlled, and not only restricted to the manufacturer's default settings. For this purpose, optimization studies are needed combining patient factors, image quality and related acceptable dose levels in controlled settings. This is a true challenge requiring well-defined anthropomorphic phantoms, surely when it comes to paediatric protocol optimization.

A potential anthropomorphic phantom should contain materials that scatter and absorb ionizing radiation in a similar way to human tissues. Furthermore, the material should not only accurately mimic soft tissues without artefacts, yet also be universally available and reproducible.³ Commercially available phantoms made with tissue equivalent materials have been used as patient substitute during *in vitro* studies.⁴ In addition, distinct materials such as water, wax, resin, paraffin and polyethylene have been proposed,^{5–8} yet those materials have not been validated and/or compared when it comes to CBCT image quality studies. Among them, wax and water were most often used in research with CBCT.^{9–12}

Human soft tissues, water and Mix-D (a mixture of paraffin wax and other chemicals) are able to yield similar X-ray transmission data, considering the very similar effective atomic number (*i.e.* soft tissues: 7.33, water: 7.42, Mix-D: 7.47).⁷ However, the volume of water surrounding the anatomic sample is difficult to control and model following a natural soft tissue contour, especially when different sizes of mandibles or skulls are scanned. This fact can bias the experiment, producing unrealistic images that do not represent the quality of clinical scans owing to differences in attenuation, scatter and beam hardening. Moreover, some factors (*e.g.* noise pattern, grey scale) can change according the amount of

tissue inside and outside the field of view in CBCT.^{13,14} In addition, anthropomorphic phantoms dedicated to radiographic training of dental students do not produce satisfactory CBCT scans for image quality assessment, and currently, only adult phantoms are available.

It can be stated that there is a true lack of standardization of the material covering the human skulls, not all materials are truly soft tissue equivalent, and some may even produce scatter artefacts along the skull. Even more important with regard to paediatric dose optimization, is the fact that age-specific paediatric skull phantoms are not commercially available. Thus, the aim of the present report was to develop age-specific paediatric anthropomorphic head phantoms for image quality and optimization studies, using Mix-D soft tissue equivalent material. The subobjective was the validation of those resulting paediatric phantoms for image quality assessment and optimization in the European DIMITRA project (*Dentomaxillofacial paediatric imaging: an investigation towards low dose radiation induced risks*).

Methods and materials

Natural skulls' features

Six paediatric skulls were obtained with ethical approval from the anatomical collection of Hasselt University (Hasselt, Belgium). The skulls were carefully selected based on age and particular pathological characteristics. To that end, skulls were visually and radiographically (panoramic radiographs) examined in order to estimate their ages according to the dental development. [Table 1](#) recaps the age estimation (from 4 to 10 years old) as well as particular clinical and radiographic findings, allowing studies on diagnostic image quality.

All skulls were satisfactory preserved with regard to bone and dental tissues. Dental fractures and cavities were observed by means of visual inspection, and then confirmed by radiographic examinations. No large metallic restorations, dental posts or implants were present. Several dental germs (normal or malpositioned), some missing teeth and a mesiodens were also

Table 1 Age estimation of the skulls and the remarkable radiographic findings

| Phantom | Age estimation | Radiographic findings |
|---------|----------------|---|
| 1 | 4–5 years old | Dental fractures, dental germs in malposition |
| 2 | 5 years old | Dental fractures, dental germs in malposition |
| 3 | 6 years old | Dental fractures |
| 4 | 7–8 years old | Dental fractures, missing teeth |
| 5 | 8–9 years old | Dental cracks, malposition of dental germs, mesiodens |
| 6 | 9–10 years old | Dental cracks, dental follicle enlargement, dental decay, root resorption (external and internal) |

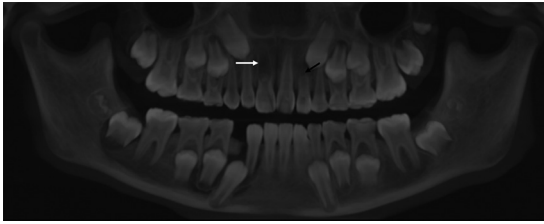


Figure 1 Panoramic reconstruction of skull 6. The white arrow indicates an internal resorption of the root of the right central incisor and the black arrow points out an external root resorption (apical third) of the left lateral incisor, possibly triggered by the deviation of the canine eruption pathway.

detected. Furthermore, one skull also presented internal and external dental resorptions in the upper right central incisor and upper left lateral incisor (Figure 1).

Soft tissue equivalent Mix-D preparation

The Mix-D preparation was adapted from the study of Brand *et al*⁷ that described a phantom for radiation dosimetry, using the original recipe introduced by Jones and Raine in 1949.¹⁵ For the present project, 500 g of Mix-D was prepared in fractionated portions of 304 g of paraffin wax, 152 g of polyethylene, 32 g of magnesium oxide and 12 g of titanium dioxide. First, the wax, magnesium oxide and titanium dioxide were weighted, mixed and melted together (105 °C) in a glass round flask with a sufficient diameter to immerse the largest skull. When the preparation was fully melted and mixed, polyethylene was added and the mixture heated for another 20 min. The Mix-D manipulation procedure—preparation and skull covering—was carried out in a fume hood to assure chemical safety.

Skull covering

Before the immersion process, skulls were protected with crepe tape (paper with adhesive resin–rubber-based, 24 mm width; 3 M, Maplewood, MN), especially in the areas of foraminae (mandibular, mental, skull bases), large cavities (orbital, foramen magnum) and teeth (Figure 2a,b). This procedure avoids excessive infiltration of the melted material inside the cranial cavities as well as through the interdental spaces.

For craniofacial covering, the skulls were held by the cranial bones and immersed in the melted preparation up to the superior orbital arch (Figure 2c). When the Mix-D presented the typical loss of gloss indicating a predrying of the external surface, the skull was reimmersed. This procedure was repeated several times until the achievement of a consistent and uniform layer of Mix-D surrounding the skull. After 24 h, skulls were immersed in an inverted position, holding them in the zygomatic arches areas. The mandibles were covered separately holding the condyles and wrapped up to the cervical limit of the teeth (Figure 2d). The inverted immersion was also performed after 24 h, in order to cover condyles, ramus and coronoid processes. Finishing and refinement procedures were conducted with heated

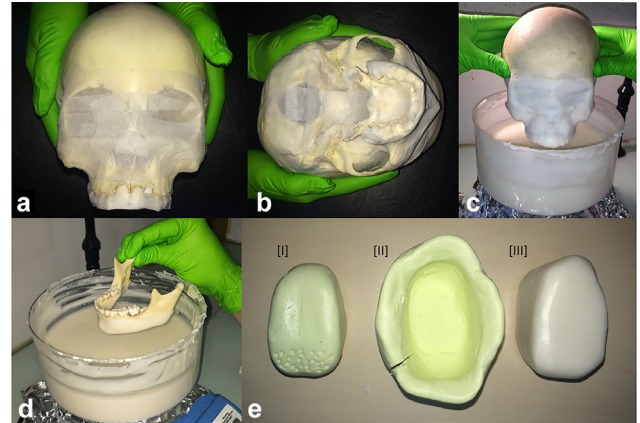


Figure 2 The skulls were first covered with paper crepe-tape, mainly in the teeth and cavities, in order to avoid overflowing of Mix-D (a, b). (c, d) show the “layer after layer” immersion procedure for skulls and mandibles embedding, that took place in a round glass recipient, under continuous low heating. A Mix-D tongue was also made (e-III) through a silicone model (e-I) and an impression (e-II) that was filled up with melted Mix-D.

carving tools in order to remove excess of Mix-D that have infiltrated in interdental spaces or appeared attached to the dental surfaces. Finally, to include X-ray attenuation generated by soft tissue of the tongue, a model of the tongue was shape in Mix-D from a silicon cast (Figure 2e).

CBCT scanning

For validation purposes, the six resulting paediatric phantoms were scanned using two CBCT units with different exposure parameter settings (CS9300, Carestream, Rochester, NY and NewTom Giano, NewTom, Verona, Italy). This allowed checking for artefact-free alignment of the Mix-D onto the bony surface, with adequate thickness and homogeneous layering, thus mimicking human soft tissues, as made visible on CBCT. Preliminary images deriving from all scans were evaluated by two dentomaxillofacial radiologists, to check for air bubbles, artefacts and inhomogeneity’s of the Mix-D and a potential effect on the jaw bone. Only skulls presenting perfect alignment of Mix-D surrounding the bone surfaces with adequate and realistic soft tissue thickness density were accepted.

Results

Six DIMITRA paediatric phantoms (4- to 10-year-old skulls) with Mix-D soft tissue equivalent material have been prepared (Figure 3); Figure 4 allows a detailed view of phantom number 3. Figure 5 shows a set of CBCT images obtained from the DIMITRA phantoms on the CS9300 unit with large fields of view (17 × 11 cm in a–c; 10 × 10 cm in d–f). It is possible to note the perfect alignment of the Mix-D surrounding the bone surfaces as well as the material thickness and density compatible with the soft tissue aspect observed through *in vivo* CBCT exams.

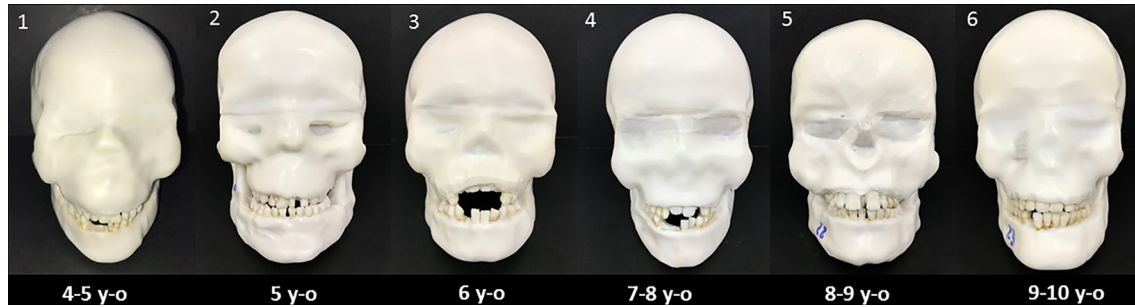


Figure 3 The six DIMITRA age-specific paediatric phantoms.

There was a slight entry of melted Mix-D inside large bone cavities, mainly orbits, maxillary sinus and nasal cavity. However, there were no gaps between Mix-D and bone structures and resulting images were found mimicking clinical conditions.

Figure 6 allows a comparison between CBCT scans obtained from a DIMITRA phantom under different exposure and reconstruction parameters (a–c) and from a child that presented a clinical indication for a three-dimensional exam. The general similarity and close grey levels of the Mix-D images (a–c) and the soft tissue aspect (d) can be noted. Other highlights include



Figure 4 Phantom number 3, representing a child of 6 years old with the upper incisors in the eruptive stage showing the first third of the crowns clinically.

the subjective visual differences related to noise and contrast patterns produced by different CBCT units and technical parameters. Nevertheless, the perfect fit of the Mix-D to the bone surfaces, following the outline and bone shape, seems to create favourable conditions for image quality assessment.

Discussion

The presently introduced paediatric skull phantom collection has shown to be useful for age-specific CBCT image quality assessment and optimization. In addition, the DIMITRA paediatric phantoms showed some pathological conditions that might be useful for a number of imaging studies, not only involving optimization, but also testing other experimental issues involving two- and three-dimensional diagnostic imaging. The Mix-D preparation and embedding technique described in the present report appears to be practical and reproducible, as long as the right chemical proportion,

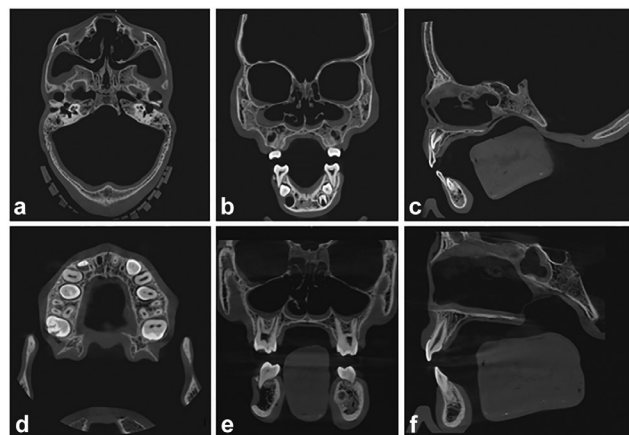


Figure 5 CBCT images obtained on the CS9300 unit, from phantoms 1 (a–c; field of view 17×11 cm, 90 kV, 4 mA, voxel size 0.3 mm, 12 s) and 6 (d, e; a–c; field of view 10×10 cm, 90 kV, 4 mA, voxel size 0.18 mm, 8 s). The images show a perfect fit of the Mix-D over the bone surfaces and the smooth and continuous outline following the contour of the craniofacial structures. A slight overflow of Mix-D can be detected inside the cranium (a–c), maxillary sinus (b, e), sphenoid sinus (f), nasal cavity (b, c, e, f) and orbits (b, e). Axial (a, d) coronal (b, e) and sagittal views (c, f). CBCT, cone-beam CT.

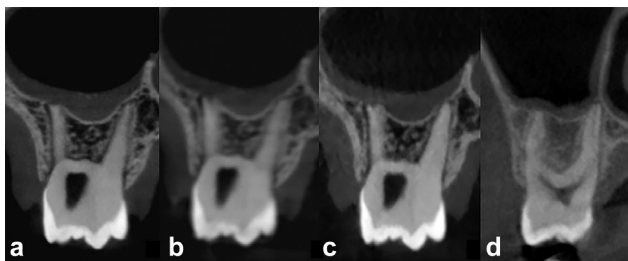


Figure 6 CBCT images of the DIMITRA phantom number 6, 9–10-year-old (a–c) and a 13-year-old boy (d) illustrating the similarity (soft tissue aspect) in different conditions (different CBCT units and technical parameters). (a) Acquired from a CS9300 unit, FOV 5 × 5 cm, 90 kVp, 5 mA, voxel size 0.09 mm, 20 s. (b) Acquired from a CS9300 unit, FOV 8 × 8 cm, 90 kVp, 5 mA, voxel size 0.18 mm, 8 s. (c) Acquired from a NewTom Giano unit, FOV 11 × 5 cm, 90 kVp, 3 mA, voxel size 0.15 mm, 9 s. (d) Performed with a ProMax 3D Max unit (Planmeca, Helsinki, Finland), FOV 5 × 5 cm, 96 kVp, 11 mA, voxel size 0.2 mm, 12 s [obtained from the clinical data collection of the authors' institution (Paris Descartes University)]. CBCT, cone-beam CT; FOV, field of view.

melting sequence and immersion technique is used. On the other hand, a drawback of the current technique is the difficulty to strictly control the thickness of Mix-D during the layer-by-layer immersion. As the melted material gets dry and solid, it is difficult to introduce some measurement tool through the surface owing to the risk of cracking. This feature also becomes apparent when drilling slots for dosimeters insertion.⁷ However, for image quality studies in which conventional dosimeters are not necessary, the present phantoms are perfectly applicable. For instance, in the DIMITRA project, paediatric dosimetry studies were performed using Monte Carlo simulation involving voxel phantoms; thus, there was no need to construct slots for dosimeters.

Some infiltration of the Mix-D could be detected, especially in large cavities like orbits and paranasal cavities. However, this material infiltration can be controlled and minimized by means of protection with non-radiopaque tape. Furthermore, the specific Mix-D infiltration in paranasal cavities may mimic some clinical pathological conditions like thickening of the sinus membrane in allergic or inflammatory processes.

It is worth mentioning that, at this moment, we did not include natural cervical vertebrae and soft tissues of the neck in the acquisitions, since matching paediatric vertebrae were not available from the University of Hasselt's anatomical collection. Therefore, it can be expected that the CBCT scans show a slight overestimation of the corresponding clinical image quality owing to a reduced X-ray attenuation from A–P and P–A

projection angles as well as a reduced amount of X-ray scatter, resulting in an increased signal-to-noise ratio at the level of the detector. However, the use of the phantoms in (ongoing) follow-up studies involved the use of a posterior support serving as a replacement for the neck, allowing for an evaluation of effects on image quality in the presence and absence of neck tissue simulation.

Despite the aforementioned limitations with regard to development of age-specific paediatric phantoms with soft tissue equivalent material, one should be aware that studies more closely approaching clinical reality are ethically not tolerated. *In vivo* studies conducted with variations of protocols and exposure factors are obviously not acceptable, especially for paediatric patients considering their higher susceptibility to stochastic effects from radiation exposures.¹⁶ So, as described above, the present phantoms are not a limitation-free model, but they represent a starting point. Moreover, the soft tissue simulation method described here can be reproduced and optimized from this first insight.

The phantoms are primarily intended for the evaluation of clinical image quality. To date, no technical image quality parameters were measured for CBCT images of the DIMITRA phantoms images such as contrast-to-noise ratio, modulation transfer function or CT number accuracy. More studies involving objective measurements in the DIMITRA phantoms are necessary in order to reinforce the preliminary subjective image quality results obtained up till now.

The rapidly changing field of CBCT technology urges the need for continuous monitoring of the resulting image quality and related radiation doses. For this reason, further research is continuously needed to allow optimization studies for clinical purposes. This may be of particular interest when it comes to paediatric imaging.

In conclusion, the DIMITRA anthropomorphic phantoms developed by means the covering of six paediatric skulls with Mix-D have shown appropriate images for dentomaxillofacial research involving CBCT. Moreover, the layer-by-layer technique described here showed to be feasible to perform, as long as all care and recommendations are followed strictly.

Funding

The research leading to these results has received funding from the European Atomic Energy Community's Seventh Framework Programme FP7/2007–2011 under grant agreement no 604984 (OPERRA: Open Project for the European Radiation Research Area).

References

1. Bushberg JT. Eleventh annual Warren K. Sinclair keynote address-science, radiation protection and NCRP: building on the

past, looking to the future. *Health Phys* 2015; **108**: 115–23. doi: <https://doi.org/10.1097/HP.0000000000000228>

2. Oenning AC, Jacobs R, Pauwels R, Stratis A, Hedesiu M, Salmon B. Cone-beam CT in paediatric dentistry: DIMITRA project position statement. *Pediatr Radiol* 2017; **118**. doi: <https://doi.org/10.1007/s00247-017-4012-9>
3. Farquharson MJ, Spyrou NM, al-Bahri J, Highgate DJ. Low energy photon attenuation measurements of hydrophilic materials for tissue equivalent phantoms. *Appl Radiat Isot* 1995; **46**: 783–90. doi: [https://doi.org/10.1016/0969-8043\(95\)00025-9](https://doi.org/10.1016/0969-8043(95)00025-9)
4. Nejaim Y, Silva AI, Brasil DM, Vasconcelos KF, Haiter Neto F, Boscolo FN. Efficacy of lead foil for reducing doses in the head and neck: a simulation study using digital intraoral systems. *Dentomaxillofac Radiol* 2015; **44**: 20150065. doi: <https://doi.org/10.1259/dmfr.20150065>
5. Richards AG, Webber RL. Constructing phantom heads for radiation research. *Oral Surg Oral Med Oral Pathol* 1963; **16**: 683–90. doi: [https://doi.org/10.1016/0030-4220\(63\)90073-2](https://doi.org/10.1016/0030-4220(63)90073-2)
6. Hildebolt CF, Rupich RC, Vannier MW, Zerbolio DJ, Shrout MK, Cohen S, et al. Inter-relationships between bone mineral content measures. Dual energy radiography (DER) and bitewing radiographs (BW). *J Clin Periodontol* 1993; **20**: 739–45. doi: <https://doi.org/10.1111/j.1600-051X.1993.tb00700.x>
7. Brand JW, Kuba RK, Braunreiter TC. An improved head-and-neck phantom for radiation dosimetry. *Oral Surg Oral Med Oral Pathol* 1989; **67**: 338–46. doi: [https://doi.org/10.1016/0030-4220\(89\)90367-8](https://doi.org/10.1016/0030-4220(89)90367-8)
8. Cook JE, Cunningham JL. The assessment of fracture healing using dual x-ray absorptiometry: a feasibility study using phantoms. *Phys Med Biol* 1995; **40**: 119–36. doi: <https://doi.org/10.1088/0031-9155/40/1/011>
9. Shelley AM, Brunton P, Horner K. Subjective image quality assessment of cross sectional imaging methods for the symphyseal region of the mandible prior to dental implant placement. *J Dent* 2011; **39**: 764–70. doi: <https://doi.org/10.1016/j.jdent.2011.08.008>
10. Melo SL, Haiter-Neto F, Correa LR, Scarfe WC, Farman AG. Comparative diagnostic yield of cone beam CT reconstruction using various software programs on the detection of vertical root fractures. *Dentomaxillofac Radiol* 2013; **42**: 20120459. doi: <https://doi.org/10.1259/dmfr.20120459>
11. Oliveira ML, Tosoni GM, Lindsey DH, Mendoza K, Tetradis S, Mallya SM. Influence of anatomical location on CT numbers in cone beam computed tomography. *Oral Surg Oral Med Oral Pathol Oral Radiol* 2013; **115**: 558–64. doi: <https://doi.org/10.1016/j.oooo.2013.01.021>
12. Lagos De Melo LP, Oenning ACC, Nadaes MR, Nejaim Y, Neves FS, Oliveira ML, et al. Influence of acquisition parameters on the evaluation of mandibular third molars through cone beam computed tomography. *Oral Surg Oral Med Oral Pathol Oral Radiol* 2017; **124**: 183–90. doi: <https://doi.org/10.1016/j.oooo.2017.03.008>
13. Oliveira ML, Freitas DQ, Ambrosano GM, Haiter-Neto F. Influence of exposure factors on the variability of CBCT voxel values: a phantom study. *Dentomaxillofac Radiol* 2014; **43**: 20140128: 20140128. doi: <https://doi.org/10.1259/dmfr.20140128>
14. Pauwels R, Jacobs R, Singer SR, Mupparapu M. CBCT-based bone quality assessment: are Hounsfield units applicable? *Dentomaxillofac Radiol* 2015; **44**: 20140238. doi: <https://doi.org/10.1259/dmfr.20140238>
15. Jones DEA, Raine HC. Letter to the editor. *Br J Radiol* 1949; **22**: 549–50.
16. White SC, Scarfe WC, Schulze RK, Lurie AG, Douglass JM, Farman AG, et al. The image gently in dentistry campaign: promotion of responsible use of maxillofacial radiology in dentistry for children. *Oral Surg Oral Med Oral Pathol Oral Radiol* 2014; **118**: 257–61. doi: <https://doi.org/10.1016/j.oooo.2014.06.001>